JOURNAL OF BACTERIOLOGY, June 2011, p. 2814–2825 Vol. 193, No. 11
0021-9193/11/$12.00 doi:10.1128/JB.00015-11

Surface Localization Determinants of *Borrelia* OspC/Vsp Family Lipoproteins▽

Ozan S. Kumru,[1] Ryan J. Schulze,[1]† Mykola V. Rodnin,[2] Alexey S. Ladokhin,[2] and Wolfram R. Zückert[1]*

Department of Microbiology, Molecular Genetics and Immunology[1] and Department of Biochemistry and Molecular Biology,[2] University of Kansas Medical Center, 3901 Rainbow Boulevard, Kansas City, Kansas 66160

Received 4 January 2011/Accepted 21 March 2011

The dimeric OspC/Vsp family surface lipoproteins of *Borrelia* spirochetes are crucial to the transmission and persistence of Lyme borreliosis and tick-borne relapsing fever. However, the requirements for their proper surface display remained undefined. In previous studies, we showed that localization of *Borrelia burgdorferi* monomeric surface lipoprotein OspA was dependent on residues in the N-terminal "tether" peptide. Here, site-directed mutagenesis of the *B. burgdorferi* OspC tether revealed two distinct regions affecting either release from the inner membrane or translocation through the outer membrane. Determinants of both of these steps appear consolidated within a single region of the *Borrelia turicatae* Vsp1 tether. Periplasmic OspC mutants still were able to form dimers. Their localization defect could be rescued by the addition of an apparently structure-destabilizing C-terminal epitope tag but not by coexpression with wild-type OspC. Furthermore, disruption of intermolecular Vsp1 salt bridges blocked dimerization but not surface localization of the resulting Vsp1 monomers. Together, these results suggest that *Borrelia* OspC/Vsp1 surface lipoproteins traverse the periplasm and the outer membrane as unfolded monomeric intermediates and assemble into their functional multimeric folds only upon reaching the spirochetal surface.

Since the original description of a prokaryotic lipoprotein in the cell envelope of *Escherichia coli* over 4 decades ago (12), this class of peripherally anchored membrane proteins has been increasingly appreciated. In diderm bacteria, lipoproteins are routed via the general secretory pathway through and to the inner membrane (IM), where they are posttranslationally modified by acylation at a conserved Cys residue (25). Sorting within the periplasm depends on variations of an N-terminal signal first identified in *E. coli* (23, 33, 40, 62, 63, 71) and is carried out by the Lol system, consisting of the IM ABC transporter-like LolCDE complex (70), the periplasmic lipoprotein carrier LolA (37), and the outer membrane (OM) lipoprotein receptor LolB (38, 72). Established pathways of lipoprotein translocation through the OM involve either a type II or type V secretion system (17, 20, 51, 52, 57, 69).

Beyond the involvement of Braun's lipoprotein Lpp in bacterial cell envelope stability, lipoproteins were shown to play roles in a variety of cellular and pathogenic processes, most recently reviewed in reference 28. In *Borrelia* spirochetes, the etiologic agents of arthropod-borne Lyme disease and relapsing fever, surface lipoproteins are particularly abundant and constitute the predominant class of known virulence factors at the vector/host-pathogen interface (5, 11, 29, 42, 74). Outer surface protein A (OspA), e.g., is expressed by the Lyme disease spirochete *Borrelia burgdorferi* during the vector phase, where its immunoprotective and adhesive properties appear to ensure continuity of the infectious cycle (6, 7, 44, 45). Upon tick feeding and transmission to a new mammalian host, complex regulatory mechanisms lead to the replacement of OspA by OspC (45, 46, 60, 61, 65, 66). OspC is required for the establishment of mammalian infection (24), which appears to be further enhanced by binding to Salp15, an immune-modulating tick salivary gland protein (2, 53). Variable small proteins (Vsps) are expressed by tick-borne relapsing fever spirochetes, such as *Borrelia turicatae*, and are phylogenetically and structurally related to OspC (19, 30, 32, 75). They contribute to chronic infection of mammalian hosts by participating in an elaborate scheme of multiphasic antigenic variation designed to repeatedly evade the host's immune response (5). Vsps have also been shown to be the determinants of *B. turicatae* tissue tropism (14, 15, 22, 48, 49) and may enhance invasion of tissues by binding to glycosaminoglycans (36).

Our previous investigations into the secretion of the major *Borrelia* surface lipoproteins led to some intriguing discoveries. We first noticed that any known OM lipoprotein secretion modules, i.e., LolB, type II or type V systems, were missing from *Borrelia* genomes. At the same time, relapsing fever *Borrelia* lipoproteins, such as Vsp1, were compatible with the *B. burgdorferi* lipoprotein secretion machinery (76). This implied a novel genus-wide mechanism for *Borrelia* OM lipoprotein targeting and translocation. Using OspA as a first-model lipoprotein, we subsequently showed that the established eubacterial sorting rules (23, 33, 40, 62, 63, 71) did not apply to borrelial lipoproteins (59). Next, we discovered that a specific region in the OspA tether region is required for efficient OM translocation and that C-terminal epitope tags of periplasmic OspA mutants were selectively displayed on the bacterial sur-

* Corresponding author. Mailing address: University of Kansas Medical Center, Department of Microbiology, Molecular Genetics and Immunology, Mail Stop 3029, 3025 Wahl Hall West, 3901 Rainbow Boulevard, Kansas City, KS 66160. Phone: (913) 588-7061. Fax: (913) 588-7295. E-mail: wzueckert@kumc.edu.

† Present address: Department of Biochemistry, University of Bristol School of Medical Sciences, University Walk, Bristol BS8 1TD, United Kingdom.

▽ Published ahead of print on 25 March 2011.

face. Additional OspA mutants indicated that the above-described tether mutations lead to premature folding of OspA in the periplasm (58). This suggested that lipoprotein translocation through the outer spirochetal membrane requires an unfolded conformation of the substrate protein and can initiate at the C terminus yet is independent of a specific C-terminal-targeting peptide.

In this report, we expanded our studies to the OspC/Vsp family of proteins, which form dimeric α-helical bundles with proximal N and C termini (19, 30, 32, 75). As such, they are structurally distinct from the OspA β-sheet monomer, where the C terminus is distal from the N-terminal membrane anchor (8, 34). The data now allow us to compare and contrast the secretion requirements of two different *Borrelia* surface lipoprotein folds.

MATERIALS AND METHODS

Bacterial strains and growth conditions. *Borrelia burgdorferi* B313 (56), B31-A3 *ospC*::*kanR* (provided by P. Rosa, NIH/NIAID Rocky Mountain Laboratories, Hamilton, MT), and B31-e2 (provided by B. Stevenson, University of Kentucky, Lexington, KY [3]) are all derivatives of strain B31 (ATCC 35210). B313 contains plasmids cp26, cp32-1, cp32-2/7, cp32-3, and lp17 (76, 77). B31-e2 contains plasmids cp26, cp32-1, cp32-3, cp32-4, lp17, lp38, and lp54 (3). The B31-A3 *ospC*::*kanR* strain is a low-passage, transformable clone lacking lp25 (not shown). *B. burgdorferi* cells were cultured in liquid or solid Barbour-Stoenner-Kelly II (BSK-II) medium at 34°C under a 5% CO_2 atmosphere (4, 73). Selective BSK-II media were supplemented where needed with 200 μg/ml of kanamycin or 50 μg/ml of streptomycin (Sigma). *E. coli* strains TOP 10 (Invitrogen) and XL-10 Gold (Stratagene) were used for plasmid construction and propagation, and BL21(DE3) pLysS was used for recombinant protein expression. Unless noted otherwise, *E. coli* cultures were grown at 37°C in LB broth or LB agar (Difco) supplemented with 30 μg/ml of kanamycin or 100 μg/ml spectinomycin (Sigma), respectively.

Site-directed mutagenesis. Plasmids carrying mutant genes (Table 1) were constructed either by splicing overlap extension PCR (SOE-PCR) (26) with Pfx Platinum (Invitrogen) or Phusion Hot Start (New England BioLabs) thermostable proofreading DNA polymerase or by following the Quick-Change site-directed mutagenesis protocol (Stratagene), using oligonucleotides listed in Table 2. Sequences were verified by DNA sequencing (ACGT Inc., Wheeling, IL, or Northwestern University, Chicago, IL).

SDS-PAGE and immunoblot analysis. Proteins were separated by sodium dodecyl sulfate-12.5% polyacrylamide gel electrophoresis (SDS-PAGE) and visualized by Coomassie blue staining. For immunoblots, proteins were electrophoretically transferred to Immobilon-NC nitrocellulose membranes (Millipore) using a Transblot semidry transfer cell (Bio-Rad). Membranes were rinsed in 20 mM Tris, 500 mM NaCl, pH 7.5 (TBS). TBS with 0.05% Tween 20 (TBST) containing 5% dry milk was used for membrane blocking and subsequent incubation with primary and secondary antibodies; TBST alone was used for the intervening washes. Antibodies used were anti-mRFP1 (monomeric red fluorescent protein) rabbit polyclonal antiserum (16) (1:5,000 dilution; a gift from P. Viollier, University of Geneva, Switzerland), anti-OppAIV rabbit polyclonal antiserum (10) (1:100 dilution; a gift from P. A. Rosa, NIH/NIAID Rocky Mountain Laboratories, Hamilton, MT), anti-FlaB rat polyclonal antiserum (1) (1:4,000 dilution; a gift from M. Caimano, University of Connecticut Health Center, Farmington, CT), anti-OspA mouse monoclonal antibody (6) (H5332; 1:50 dilution), OspC mouse monoclonal antibody (39) (1:50 dilution; a gift from R. Gilmore via B. Stevenson, University of Kentucky, Lexington, KY), and Vsp1 mouse monoclonal (13) (1H12; 1:25 dilution) and polyclonal (71) (1:500 dilution) antibodies. Secondary antibodies were alkaline phosphatase-conjugated mouse anti-rabbit IgG (γ-chain specific), goat anti-mouse IgG (H+L), or rabbit anti-rat IgG (H+L) (Sigma). Alkaline phosphatase substrates were 1-Step NBT/BCIP (nitroblue tetrazolium–5-bromo-4-chloro-3′-indolylphosphate *p*-toluidine; Pierce) for colorimetric and CDP-Star (GE Healthcare Life Sciences) for chemiluminescent detection. Restore Western blot stripping reagent (Pierce) was used to remove bound antibodies from immunoblots to allow for reprobing of membranes. Proteins tagged with a hexahistidine epitope tag were detected directly with a nickel-activated HisProbe-horseradish peroxidase (HRP) conjugate and SuperSignal HRP chemiluminescent detection substrate (Pierce).

Protein localization assays. To distinguish between surface-displayed and subsurface proteins, intact *B. burgdorferi* cells were "shaved" by incubation of intact cells with proteinase K (*in situ* surface proteolysis) as described previously (13, 59). Endogenously expressed wild-type OspA and FlaB protein served as surface and subsurface controls, respectively. To determine the membrane localization of subsurface proteinase K-resistant proteins, OM vesicles were isolated by treatment of *B. burgdorferi* cells with low pH, hypotonic citrate buffer followed by isopycnic sucrose gradient ultracentrifugation as described previously (59, 64). OspA and OppAIV served as OM and IM controls, respectively.

Trypsin proteolysis assays. To test the sensitivity of OspC to trypsin, cells were incubated with 200 μg ml^{-1} of trypsin (Sigma) as described previously (13). To gain access to periplasmic OspC proteins, cells were treated with 0.1% SDS to permeabilize the OM (Sigma) (27). Surface-localized OspC released into the reaction supernatant was fractionated from cell-associated OspC by centrifugation as described previously (75). Proteins present in the supernatant were precipitated with ice-cold acetone. Both pellet and supernatant samples were resuspended in equal volumes of SDS-PAGE sample buffer and loaded in equivalent ratios.

***In situ* cross-linking.** Assays were carried out as described previously (13, 75). Briefly, cells were grown to a density of about 5×10^7 cells/ml, harvested, and washed twice in phosphate-buffered saline (PBS) plus Mg. Proteins were cross-linked with 1% (vol/vol) formaldehyde (Sigma) at room temperature for 30 min. Cells were washed twice with PBS plus Mg, resuspended in SDS-PAGE loading dye with 50 mM dithiothreitol (DTT), and incubated at 37°C for 10 min before separation of whole-cell proteins by SDS-PAGE.

Purification of recombinant OspC. DNA fragments corresponding to N-terminally truncated, soluble OspC were amplified by PCR from pOSK307 (Table 1) with oligonucleotide primers, including 5′ NdeI and 3′ BamHI extensions (Table 2). The three different 5′ oligonucleotide primers placed the N20, N31, and V37 codons immediately after the formylmethionyl (fMet) start codon, respectively. The PCR products were gel purified, digested with NdeI and BamHI, and ligated with a pET29b (Novagen) backbone previously linearized with NdeI and BamHI. The resulting expression plasmids were sequenced and used to transform BL21(DE3) pLysS (Novagen). A 1:100 dilution of an overnight culture grown at 37°C in LB containing 30 μg ml^{-1} kanamycin and 100 μg ml^{-1} chloramphenicol was used to inoculate a larger culture of selective Terrific broth. After cultivation at 37°C to an optical density at 545 nm (OD_{545}) of 0.3 to 0.4, recombinant protein expression was induced with 1 mM isopropyl-β-D-1-thiogalactopyranoside (Invitrogen) for 5 h at 30°C. Cells were harvested and lysed by sonication, and cell debris was removed by centrifugation at 12,000 × *g* for 20 min at 4°C. The cell-free lysate was then applied to a Talon cobalt column (Clontech) equilibrated with loading buffer (300 mM NaCl, 50 mM $NaPO_4$, pH 7.0) and washed with loading buffer containing 10 mM imidazole. Recombinant OspC at a purity of about 90% was eluted in buffer containing 100 mM imidazole (Sigma). For further purification, we followed the protocol described in reference 30 with some modifications. The cobalt column eluate was dialyzed twice against 20 mM $NaPO_4$ and 5 mM NaCl, pH 7.7, and then applied to a Hi-Trap Q anion-exchange column (GE Healthcare). The flowthrough containing OspC was dialyzed twice against 10 mM $NaPO_4$ and 5 mM NaCl, pH 6.0, and applied to a Hi-Trap SP cation-exchange column (GE Healthcare). OspC eluted quantitatively at 500 mM NaCl at a purity of about 98% and was dialyzed twice against 10 mM $NaPO_4$ buffer, pH 7.0, and concentrated using Amicon Ultra centrifugal filters with a 3-kDa cutoff (Millipore). Protein concentrations were determined by Bradford assay (Bio-Rad).

Circular dichroism measurements and analysis of thermal unfolding. Circular dichroism measurements were performed using an upgraded Jasco-720 spectropolarimeter (Japan Spectroscopic Company, Tokyo, Japan). Ten to twenty scans were recorded between 190 and 260 nm with a 1-nm step at +20°C, using a 1-mm optical path cuvette. $rOspC_{N20}$, $rOspC_{N31}$, and $rOspC_{V37}$ protein concentrations of 3 to 5 μM, determined by UV absorbance measurements using a coefficient of molar extinction of 2,400 M^{-1} cm^{-1}, were used in the experiments. All spectra were corrected for background. Temperature dependencies of unfolding were measured at 222 nm, with a 1-degree/min scan rate. Thermal unfolding was analyzed as described previously (18) to obtain transition temperature (T_m) and enthalpy (ΔH). The free energy (ΔG) stabilizing native structure at room temperature was estimated using standard assumptions on the value of heat capacity according to Robertson and Murphy (54).

RESULTS

OspC/Vsp1 localization determinants are also confined to the tether, but minimal tether requirements differ from those of OspA. In two previous studies, we determined the N-termi-

TABLE 1. Bacterial strains and plasmids used in this study

Strain/plasmid	Description	Source/reference
Strains		
Borrelia burgdorferi		
B313	Clone of B31 ATCC 35210 (cp26, cp32-1, cp32-2/7, cp32-3, and lp17)	55
B31e2	Clone of B31 ATCC 35210 (cp26, cp32-1, cp32-3, cp32-4, lp17, lp38, and lp54)	3
B31-A3 (Δ*ospC*)	Outer surface protein C (*ospC*) knockout, P_{flaB}-*kan* insertion in *ospC* ($lp25^-$)	K. Tilly and P. A. Rosa, unpublished
Escherichia coli		
Top10	F^- *mcrA* Δ(*mrr-hsdRMS-mcrBC*) ϕ80*lacZ*ΔM15 Δ*lacX74 recA1 araD139* Δ(*ara leu*)*7697 galU galK rpsL* (Str^r) *endA1 nupG*	Invitrogen
XL-10 Gold	Tet^r Δ(*mcrA*)*183* Δ(*mcrCB-hsdSMR-mrr*)*173 endA1 supE44 thi-1 recA1 gyrA96 relA1 lac* The F′ *proAB* $lacI^qZ$ΔM15 Tn*10* (Tet^r) Amy Cam^r	Stratagene
BL21(DE3) pLysS	F^- *ompT* $hsdS_B(r_B^- m_B^-)$ *gal dcm* λ(DE3) *tonA* pLysS (Cam^r)	Novagen
Plasmids		
pET29b	Expression vector for protein purification	Novagen
pVsp1	pBSV2::PflaB-vsp1	75
pBSV2	Shuttle vector (Kan^r)	67
pKFSS1	Shuttle vector (Str^R)	21
pRJS1091	pBSV2::PflaBospA22-mRFPΔ4	This study
pRJS1090	pBSV2::PflaBospA25-mRFPΔ4	This study
pOSK240	pBSV2::PflaBospC29-mRFPΔ4	This study
pOSK258	pBSV2::PflaBospC30-mRFPΔ4	This study
pOSK257	pBSV2::PflaBvsp1-31-mRFPΔ4	This study
pOSK256	pBSV2::PflaBvsp1-32-mRFPΔ4	This study
pOSK200	pKFSS1::PflaB-ospC	This study
pOSK273	pKFSS1::PflaBospC(ΔN20-A30)	This study
pOSK274	pKFSS1::PflaBospC(ΔN31-N41)	This study
pOSK299	pKFSS1::PflaBospC(ΔS22)	This study
pOSK300	pKFSS1::PflaBospC(ΔN21)	This study
pOSK287	pKFSS1::PflaBospC(ΔN20-S22)	This study
pOSK288	pKFSS1::PflaBospC(ΔG23-D25)	This study
pOSK301	pKFSS1::PflaBospC(ΔN21-S22)	This study
pOSK294	pKFSS1::PflaBospC(ΔA33-N41)	This study
pOSK302	pKFSS1::PflaBospC(ΔD34-N41)	This study
pOSK309	pKFSS1::PflaBospC(Ala)21-22	This study
pOSK310	pKFSS1::PflaBospC(Gly)21-22	This study
pOSK268	pBSV2::PflaBvsp1(ΔN20-S25)	This study
pOSK269	pBSV2::PflaBvsp1(ΔG23-D28)	This study
pOSK262	pBSV2::PflaBvsp1(ΔN20-S22)	This study
pOSK263	pBSV2::PflaBvsp1(ΔG23-S25)	This study
pOSK275	pBSV2::PflaBvsp1(ΔN20-A32)	This study
pOSK276	pBSV2::PflaBvsp1(ΔK33-I39)	This study
pOSK279	pBSV2::PflaBvsp1(ΔN21-S25)	This study
pOSK278	pBSV2::PflaBvsp1(ΔS22-S25)	This study
pOSK284	pBSV2::PflaBvsp1(ΔN20-G23)	This study
pOSK285	pBSV2::PflaBvsp1(ΔN20-T24)	This study
pOSK289	pBSV2::PflaBvsp1(ΔS22-S25)	This study
pOSK291	pBSV2::PflaBvsp1(ΔN21-G23)	This study
pOSK292	pBSV2::PflaBvsp1(ΔS22-T24)	This study
pOSK313	pBSV2::PflaBvsp1(ΔN20-S25)P26A	This study
pOSK351	pET29b::pT7ospCN20-His	This study
pOSK352	pET29b::pT7ospCN31-His	This study
pOSK353	pET29b::pT7ospCV37-His	This study
pOSK248	pBSV2::PflaB-vsp1D60K/D87K/D150K	This study
pOSK307	pKFSS1::PflaB-ospC-linker-his tag	This study
pOSK312	pKFSS1::PflaB-ospC-(ΔS22)-linker-His tag	This study

nal lipopeptides required for surface localization of monomeric OspA in fusions to the red fluorescent reporter protein mRFP1. Using a standard protocol, which combined *in situ* proteolysis of intact cells to distinguish between surface and periplasmic lipoproteins with the analysis of OM vesicle (OMV) fractions to localize periplasmic lipoproteins to either the IM or OM (see Materials and Methods), we originally concluded that five N-terminal residues of the mature OspA lipoprotein were required for surface localization of mRFP1. OspA20::mRFP1, providing only four OspA tether residues, was protected from proteinase K digestion, i.e., localized largely to the periplasm, while fusions of mRFP1 to OspA21 and longer lipopeptides were protease accessible, i.e., surface displayed (59). However, we later determined that four N-terminal amino acids of mRFP1 contributed to the process and switched to a truncated mRFP1 reporter, mRFPΔ4 (58). To

TABLE 2. Oligonucleotides used in this study

Name	Sequence (5′ to 3′)[a]	Description
ospCcp26-fwd	AAGGAGGCACAAATTAATG	Forward primer to amplify *ospC* from cp26
ospCcp26-rev	AATTTGCCAAAACCGTTTAAGC	Reverse primer to amplify *ospC* from cp26
BamPflaB-fwd	CGGGATCCTGTCTGTCGCCTCTTG	Forward flanking primer for cloning with BamHI site
pBSVospC-rev	AAACGACGGCCAGTGCCAAG	Reverse flanking primer for cloning
ospCpfaB-fwd	TAAATTTTATCATGGAGGAATGACATATGAAAAAGAATACATTAAG	Forward primer to fuse *ospC* to the *flaB* promoter
ospCpfaB-rev	GTCATTAATATTGCACTTAATGTATTCTTTTTCATATGTCATTCC	Reverse primer to fuse *ospC* to the *flaB* promoter
240-fwd	ATGGGAATACATCTGACGTCATCAAGGAGTTCATGCGCTTCAAGG	Forward primer to fuse pfaB-ospC29 to mRFPΔ4
240-rev	CGCATGAACTCCTTGATGACGTCAGATGTATTCCCATCTTTC	Reverse primer to fuse pfaB-ospC29 to mRFPΔ4
258-fwd	GAAAGATGGGAATACATCTGCTGACGTCATCAAGGAGTTCATG	OspC30::mRfPΔ4 forward mutagenic primer
258-rev	CATGAACTCCTTGATGACGTCAGCAGATGTATTCCCATCTTTC	OspC30::mRfPΔ4 reverse mutagenic primer
257-fwd	GATGGGAATACATCTGCAAATGACGTCATCAAGGAGTTCATG	Vsp1-31::mRfPΔ4 forward mutagenic primer
257-rev	GAACTCCTTGATGACGTCATTTGCAGATGTATTCCCATCTTTC	Vsp1-31::mRfPΔ4 reverse mutagenic primer
256-fwd	GATGGGAATACATCTGCAAATTCTGACGTCATCAAGGAGTTCATG	Vsp1-32::mRfPΔ4 forward mutagenic primer
256-rev	GCGCATGAACTCCTTGATGACGTCAGAATTTGCAGATGTATTC	Vsp1-32::mRfPΔ4 reverse mutagenic primer
273-fwd	CTTTATTTTTATTTATATCTTGTAATTCTGCTGATGAGTCTGTTAAAG	$OspC_{\Delta 20\text{-}30}$ forward mutagenic primer
273-rev	CTTTAACAGACTCATCAGCAGAATTACAAGATATAAATAAAAATAAAG	$OspC_{\Delta 20\text{-}30}$ reverse mutagenic primer
274-fwd	GATGGGAATACATCTGCACTTACAGAAATAAGTAAAAAAATTACG	$OspC_{\Delta 31\text{-}41}$ forward mutagenic primer
274-rev	GTAATTTTTTTACTTATTTCTGTAAGTGCAGATGTATTCC	$OspC_{\Delta 31\text{-}41}$ reverse mutagenic primer
299-fwd	CTTGTAATAATGGGAAAGATGGGAATACATCTG	$OspC_{\Delta S22}$ forward mutagenic primer
299-rev	CAGATGTATTCCCATCTTTCCCATTATTACAAG	$OspC_{\Delta S22}$ reverse mutagenic primer
300-fwd	GACTTTATTTTTATTTATATCTTGTAATTCAGGGAAAGATG	$OspC_{\Delta N20}$ forward mutagenic primer
300-rev	CCCATCTTTCCCTGAATTACAAGATATAAATAAAAATAAAG	$OspC_{\Delta N20}$ reverse mutagenic primer
287-fwd	GACTTTATTTTTATTTATATCTTGTGGGAAAGATGGGAATACATCTG	$OspC_{\Delta 20\text{-}22}$ forward mutagenic primer
287-rev	CAGATGTATTCCCATCTTTCCCACAAGATATAAATAAAAATAAAGTC	$OspC_{\Delta 20\text{-}22}$ reverse mutagenic primer
288-fwd	CTTGTAATAATTCAGGGAATACATCTGCAAATTCTGCTGATG	$OspC_{\Delta 23\text{-}25}$ forward mutagenic primer
288-rev	CATCAGCAGAATTTGCAGATGTATTCCCTGAATTATTACAAG	$OspC_{\Delta 23\text{-}25}$ reverse mutagenic primer
301-fwd	CTTGTAATAATGGGAAAGATGGGAATACATCTG	$OspC_{\Delta 21\text{-}22}$ forward mutagenic primer
301-rev	CAGATGTATTCCCATCTTTCCCATTATTACAAG	$OspC_{\Delta 21\text{-}22}$ reverse mutagenic primer
294-fwd	GATGGGAATACATCTGCAATAAGTAAAAAAATTACGGATTC	$OspC_{\Delta 33\text{-}41}$ forward mutagenic primer
294-rev	GAATCCGTAATTTTTTTACTTATTGCAGATGTATTCCCATC	$OspC_{\Delta 33\text{-}41}$ reverse mutagenic primer
302-fwd	CATCTGCAAATTCTGCTCTTACAGAAATAAGTAAAAAAATTAC	$OspC_{\Delta 34\text{-}41}$ forward mutagenic primer
302-rev	GTAATTTTTTACTTATTTCTGTAAGAGCAGAATTTGCAGATG	$OspC_{\Delta 34\text{-}41}$ reverse mutagenic primer
309-fwd	CTTTATTTTTATTTATATCTTGTAATGCAGCAGGGAAAGATGGGAATAC	$OspC_{Ala21\text{-}22}$ forward mutagenic primer
309-rev	GTATTCCCATCTTTCCCTGCTGCATTACAAGATATAAATAAAAATAAAG	$OspC_{Ala21\text{-}22}$ reverse mutagenic primer
310-fwd	CTTTATTTTTATTTATATCTTGTAATGGGGGGGGGAAAGATGGGA ATAC	$OspC_{Gly21\text{-}22}$ forward mutagenic primer
310-rev	GTATTCCCATCTTTCCCCCCCCCATTACAAGATATAAATAAAAATAAAG	$OspC_{Gly21\text{-}22}$ reverse mutagenic primer
268-fwd	CTTATCTCTTGTCCTAAAGATGGGCAAGCAGCTAAATC	$Vsp1_{\Delta 20\text{-}25}$ forward mutagenic primer
268-rev	GATTTAGCTGCTTGCCCATCTTTAGGACAAGAGATAAG	$Vsp1_{\Delta 20\text{-}25}$ reverse mutagenic primer
269-fwd	CTCTTGTAATAATTCAGGGCAAGCAGCTAAATCTG	$Vsp1_{\Delta 23\text{-}28}$ forward mutagenic primer
269-rev	CAGATTTAGCTGCTTGCCCTGAATTATTACAAGAG	$Vsp1_{\Delta 23\text{-}28}$ reverse mutagenic primer
262-fwd	CTTTATTTTTACTTATCTCTTGTGGAACTTCTCCTAAAGATG	$Vsp1_{\Delta 20\text{-}22}$ forward mutagenic primer
262-rev	CATCTTTAGGAGAAGTTCCACAAGAGATAAGTAAAAATAAAG	$Vsp1_{\Delta 20\text{-}22}$ reverse mutagenic primer
263-fwd	CTCTTGTAATAATTCACCTAAAGATGGGCAAGCAGCTAAATC	$Vsp1_{\Delta 23\text{-}25}$ forward mutagenic primer
263-rev	GATTTAGCTGCTTGCCCATCTTTAGGTGAATTATTACAAGAG	$Vsp1_{\Delta 23\text{-}25}$ reverse mutagenic primer
275-fwd	CTTTATTTTTACTTATCTCTTGTAAATCTGATGGCACTGTTATTG	$Vsp1_{\Delta 20\text{-}32}$ forward mutagenic primer
275-rev	CAATAACAGTGCCATCAGATTTACAAGAGATAAGTAAAAATAAAG	$Vsp1_{\Delta 20\text{-}32}$ reverse mutagenic primer
276-fwd	CTTCTCCTAAAGATGGGCAAGCAGCTGACCTAGCTACAATAACTAAAA ACATTAC	$Vsp1_{\Delta 33\text{-}39}$ forward mutagenic primer
276-rev	GTAATGTTTTTAGTTATTGTAGCTAGGTCAGCTGCTTGCCCATCTTTAG GAGAAG	$Vsp1_{\Delta 33\text{-}39}$ reverse mutagenic primer
279-fwd	CTTATCTCTTGTAATAATCCTAAAGATGGGCAAGCAGCTAAATC	$Vsp1_{\Delta 21\text{-}25}$ forward mutagenic primer
279-rev	GATTTAGCTGCTTGCCCATCTTTAGGATTATTACAAGAGATAAG	$Vsp1_{\Delta 21\text{-}25}$ reverse mutagenic primer
278-fwd	CTTATCTCTTGTAATCCTAAAGATGGGCAAGCAGCTAAATCTG	$Vsp1_{\Delta 22\text{-}25}$ forward mutagenic primer
278-rev	CAGATTTAGCTGCTTGCCCATCTTTAGGATTACAAGAGATAAG	$Vsp1_{\Delta 22\text{-}25}$ reverse mutagenic primer
284-fwd	CTTATCTCTTGTACTTCTCCTAAAGATGGGCAAGCAGCTAAATC	$Vsp1_{\Delta 20\text{-}23}$ forward mutagenic primer
284-rev	GATTTAGCTGCTTGCCCATCTTTAGGAGAAGTACAAGAGATAAG	$Vsp1_{\Delta 20\text{-}23}$ reverse mutagenic primer
285-fwd	CTTTATTTTTACTTATCTCTTGTTCTCCTAAAGATGGGCAAGCAGCTA AATC	$Vsp1_{\Delta 20\text{-}24}$ forward mutagenic primer
285-rev	GATTTAGCTGCTTGCCCATCTTTAGGAGAACAAGAGATAAGTAAAAAT AAAG	$Vsp1_{\Delta 20\text{-}24}$ reverse mutagenic primer
289-fwd	GTAATAATACTTCTCCTAAAGATGGGCAAGCAGCTAAATC	$Vsp1_{\Delta 22\text{-}25}$ forward mutagenic primer
289-rev	CTTGCCCATCTTTAGGAGAAGTATTATTACAAGAGATAAG	$Vsp1_{\Delta 22\text{-}25}$ reverse mutagenic primer
291-fwd	CTTATCTCTTGTAATACTTCTCCTAAAGATGGGCAAGCAGCTAAATC	$Vsp1_{\Delta 21\text{-}23}$ forward mutagenic primer
291-rev	GCTTGCCCATCTTTAGGAGAAGTATTACAAGAGATAAG	$Vsp1_{\Delta 21\text{-}23}$ reverse mutagenic primer
292-fwd	CTTATCTCTTGTAATAATTCTCCTAAAGATGGGCAAGCAGCTAAATC	$Vsp1_{\Delta 22\text{-}24}$ forward mutagenic primer
292-rev	GATTTAGCTGCTTGCCCATCTTTAGGAGAATTATTACAAGAGATAAG	$Vsp1_{\Delta 22\text{-}24}$ reverse mutagenic primer
313-fwd	CTTATCTCTTGTGCTAAAGATGGGCAAGCAGCTAAATC	$Vsp1_{\Delta 20\text{-}25/P26A}$ forward mutagenic primer
313-rev	GATTTAGCTGCTTGCCCATCTTTAGCACAAGAGATAAG	$Vsp1_{\Delta 20\text{-}25/P26A}$ reverse mutagenic primer
351-fwd	GACTTTATTTTTATTTATACATATGAATAATTCAGGGAAAGATGGGA ATAC	$OspC_{N20}$ forward primer with NdeI site
352-fwd	CAGGGAAAGATGGGAATACACATATGAATTCTGCTGATGAGTCTGTT AAAG	$OspC_{N31}$ forward primer with NdeI site
353-fwd	CATATGAATTCTGCTGATCATATGGTTAAAGGGCCTAATCTTACAGAA ATAAG	$OspC_{V37}$ forward primer with NdeI site

Continued on following page

TABLE 2—*Continued*

Name	Sequence (5′ to 3′)[a]	Description
ospChisbamHI-rev	CGGGATCCTTAATGATGGTGATGATGATGAG	Reverse primer to amplify OspC-His with BamHI site
245-fwd	GCTAAGAGTGTTAAAAAGGTTCATACTTTAGTTAAATC	$Vsp1_{D60K}$ forward mutagenic primer
245-rev	GATTTAACTAAAGTATGAACCTTTTTAACACTCTTAGCAAAAG	$Vsp1_{D60K}$ reverse mutagenic primer
246-fwd	GCCAATGGTCTTGAAACTAAGGCTGATAAGAATG	$Vsp1_{D87K}$ forward mutagenic primer
246-rev	GCATTCTTATCAGCCTTAGTTTCAAGACCATTGG	$Vsp1_{D87K}$ reverse mutagenic primer
247-fwd	GACAGCTGATCTTGGTAAAAAGGATGTTAAGG	$Vsp1_{D150K}$ forward mutagenic primer
247-rev	CAGCATCCTTAACATCCTTTTTACCAAGATCAGCTGTCTTTG	$Vsp1_{D150K}$ reverse mutagenic primer

[a] Endonuclease restriction sites are underlined.

enable direct comparison of OspA and OspC/Vsp1 data, we revisited the OspA tether requirements and fused OspA21, OspA22, and OspA25 to mRFPΔ4. As expected, the requirement shifted to longer OspA-derived lipopeptides: in contrast to the mRFP1 fusions, OspAV21 (not shown) and OspAS22 tethers no longer were sufficient for surface exposure of mRFPΔ4; only OspA25::mRFPΔ4 remained surface exposed (Fig. 1A and 2A). This indicated that nine N-terminal residues of mature OspA are sufficient for surface exposure.

As for OspA, fusions with OspC and Vsp1 full-length tether peptides were able to guide mRFPΔ4 properly through the spirochetal cell envelope and to the surface (Fig. 1 and 2B and C). However, fusions to truncated OspC and Vsp1 tethers revealed some interesting differences. First, the minimal surface localization requirements were extended to tethers 12 and 14 amino acids in length, respectively. OspC30::mRFPΔ4 and Vsp1.32::mRFPΔ4 were displayed on the surface, while OspC29::mRFPΔ4 and Vsp1.31::mRFPΔ4 localized to the periplasm (Fig. 2B and C). Longer and shorter tether fusion data were consistent with these surface-to-subsurface transitions (not shown). In context with the previously published OspA-derived data (58, 59), these experiments corroborated a common tether-dependent secretion pathway for *Borrelia* surface lipoproteins, which yet appears to tolerate significant primary sequence diversity.

Tether mutagenesis reveals two separate OspC domains required for OM and surface targeting. Based on the fluorescent protein fusion data described above, we deleted the N-terminal OspC and Vsp1 peptide sequences deemed dispensable or essential for surface localization. Tetherless $OspC_{\Delta 20\text{-}41}$ and $Vsp1_{\Delta 20\text{-}39}$ mutants had a null phenotype, i.e., no protein was detected. As expected, deletion of the essential, anchor-proximal OspC tether peptide led to a defect: $OspC_{\Delta 20\text{-}30}$ remained protected from surface proteolysis with proteinase K yet fractionated to the OMV fraction like wild-type OspA or OspC and unlike the IM OppAIV control (Fig. 3). We therefore concluded that $OspC_{\Delta 20\text{-}30}$ localized predominantly to the periplasmic leaflet of the OM. Surprisingly, the deletion of the dispensable anchor-distal $OspC_{31\text{-}41}$ peptide also resulted in a sorting defect, with data indicating that the mutant protein distribution was shifted significantly toward the IM (Fig. 3B). Expansion of the tether by three residues in $OspC_{\Delta 34\text{-}41}$ was required to restore surface localization. The smallest alterations leading to mislocalization of OspC were either single or double amino acid deletions in the +3 and +4 positions. $OspC_{\Delta N21}$, $OspC_{\Delta S22}$, and $OspC_{\Delta N21/S22}$ localized to the periplasmic leaflet of the OM. Replacement of the two residues with either Gly or Ala dipeptides led to phenotypes already observed with OspA (54): Ala-Ala in $OspC_{N21A/S22A}$ was permissive for surface exposure, while Gly-Gly in $OspC_{N21G/S22G}$ prevented proper translocation through the OM. With the exception of a triple +2/+3/+4 position residue deletion in $OspC_{\Delta 20\text{-}22}$, deletions elsewhere within the tether did not affect OspC surface localization (Fig. 3).

Vsp1 tether deletion data tracked the mRFPΔ4 fusion data (Fig. 4): $Vsp1_{\Delta 33\text{-}39}$ remained surface exposed, while $Vsp1_{\Delta 20\text{-}32}$ was retained in the periplasm. A six-residue region (Asn20 to Ser25) proximal to the N-terminal cysteine proved important for proper localization. Deletion of at least four of these six residues led to an OM translocation defect, localizing the respective mutants to the periplasmic leaflet of the OM. Its full deletion in $Vsp1_{\Delta 20\text{-}25}$ led to retention in the IM. Yet, replacing the Pro residue in the +2 position with Ala in $Vsp1_{\Delta 20\text{-}25/P26A}$ restored release from the IM to the periplasmic leaflet of the OM. Other deletions within the Vsp1 tether did not affect the surface phenotype (Fig. 4B). Together, these experiments suggested that functional surface display of *Borrelia* lipoproteins required a subset of common tether amino acid residues, albeit with no stringent positional constraints relative to the N-terminal cysteine.

Interestingly, an additional lower-molecular-weight protein band can be observed with OspC and Vsp1 mutants localizing to the periplasm (Fig. 3 and 4). In a separate study (O. S. Kumru, I. Bunikis, I. Sorokina, S. Bergström, and W. R. Zückert, submitted for publication), we were able to demonstrate that these lower-molecular-weight species are due to C-terminal cleavage by the periplasmic protease CtpA (43). CtpA cleavage can be stimulated by periplasmic retention of the substrate or by addition of a C-terminal epitope tag (see also Fig. 6 and 7).

Tether peptides do not affect overall protein thermodynamic stability. Several prior studies using maltose binding protein had shown that its N-terminal signal peptide retarded protein folding to favor interactions with the SecB chaperone, thereby ensuring efficient secretion through the inner membrane Sec machinery (9, 35, 47). We therefore decided to test whether the OspC tether had similar intrinsic destabilizing capabilities. Recombinant nonlipidated OspC variants were purified, and their folded state was monitored over a temperature range from 25°C to 95°C by circular dichroism (CD) spectroscopy. Three recombinant OspC (rOspC) variants were analyzed: $rOspC_{N20}$ contained the full-length tether, replacing the N-terminal Cys with an fMet. $rOspC_{N31}$ and $rOspC_{V37}$ lacked 11 and 17 N-terminal amino acids, respectively; a deletion identical to the one in $rOspC_{N31}$ had resulted in the mislocalization of $OspC_{\Delta 20\text{-}30}$ to the periplasm *in vivo* (Fig. 3). Circular dichro-

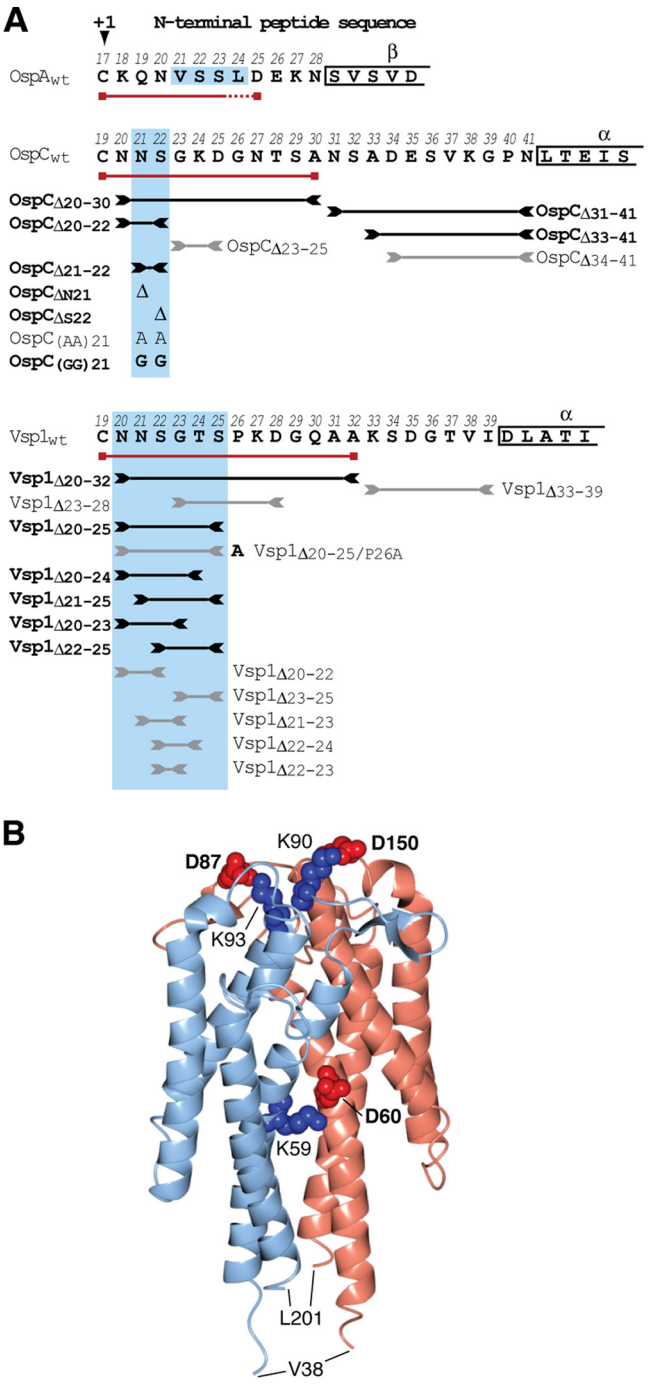

FIG. 1. Genotypes and phenotypes of OspC and Vsp1 mutants. (A) N-terminal sequences of mature lipoproteins OspA, OspC, and Vsp1 are shown in single-letter amino acid code. The +1 position Cys residue is marked with an arrowhead. Numbers above the residues indicate their positions in the prolipoprotein, including the cleaved signal peptide. Greek letters above boxed residues indicate secondary structure elements as determined by X-ray crystallography (19, 30, 32, 34). Red lines with boxed ends underline the minimum tether sequences required for surface localization of mRFPΔ4. Lines flanked by inverted arrowheads span the peptides deleted in the respective tether mutants. Black lines/bold letters mark mutants with non-wild-type phenotypes. Gray lines/regular letters mark mutants with a wild-type phenotype. Boxes shaded in light blue indicate the essential tether motifs of OspA, OspC, and Vsp1. Mutant nomenclature follows that of earlier publications (58, 59). Briefly, modified residues are numbered according to their prolipoprotein positions; numbers in lipoprotein tether-reporter fusions indicate the C-terminal tether residues present in the fusions. (B) A ribbon representation of the Vsp1 tertiary structure (Protein Data Bank ID 2GA0) (32) was generated using the CCP4 software for Macintosh (version 2.4.3) (50). The two Vsp1 chains are colored light blue and pink. Residues involved in salt bridging of the monomers are highlighted in red (Asp) or blue (Lys) spheres representing the Cα and side chain atoms. The bolded residues were mutated to yield the Vsp1 monomer. Val[38] and Leu[201] are the first and last residues visible in the crystal structure.

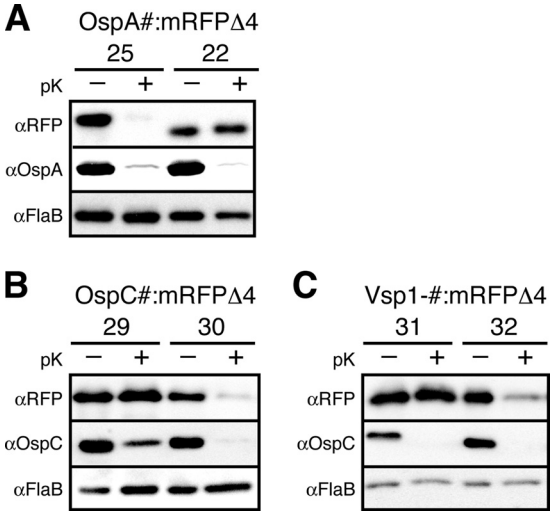

FIG. 2. Minimal OspA, OspC, and Vsp1 tether sequence requirements for surface display of the mRFPΔ4 reporter. Proteinase K (pK) accessibility immunoblots of OspA (A), OspC (B), and Vsp1 (C) tether fusions to mRFPΔ4 compared with that of $OspA_{wt}$ or $OspC_{wt}$. FlaB is used as a periplasmic, protease-resistant control. Pound signs (#) in the top-level lane descriptors are placeholders for the mutant-specific variables specified on the secondary level below (i.e., 25 on the secondary level corresponds to OspA25::mRFPΔ4).

ism spectra did not reveal any significant secondary structure variations between the three proteins (Fig. 5A). Thermal denaturation curves of all three proteins were virtually identical and had a single transition state at about 50°C (Fig. 5B and Table 3). This indicated that mutations within the tether, in the absence of other cellular proteins, resulted only in marginal changes in thermodynamic stability.

OspC mislocalized to the periplasm folds and dimerizes. We previously found that C-terminal secondary-structure-destabilizing mutations in OspA were able to overcome a tether-based mislocalization defect (58), and we interpreted this as a requirement for OspA to remain at least partially unfolded prior to translocation through the OM. Consequently, we surmised that premature folding leads to periplasmic retention of otherwise surface-displayed lipoproteins. To further test this hypothesis, we determined the folding status of two periplasmic OspC mutants, $OspC_{\Delta 20\text{-}30}$ and $OspC_{\Delta 31\text{-}41}$. A first approach built on earlier observations that the tight α-helical bundles of wild-type OspC and Vsp1 left only the proteins' N and C termini susceptible to trypsinolytic attack, while the protein cores were trypsin resistant (19, 30, 32, 75). The maintenance of a trypsin-resistant, N- and C-terminally trimmed

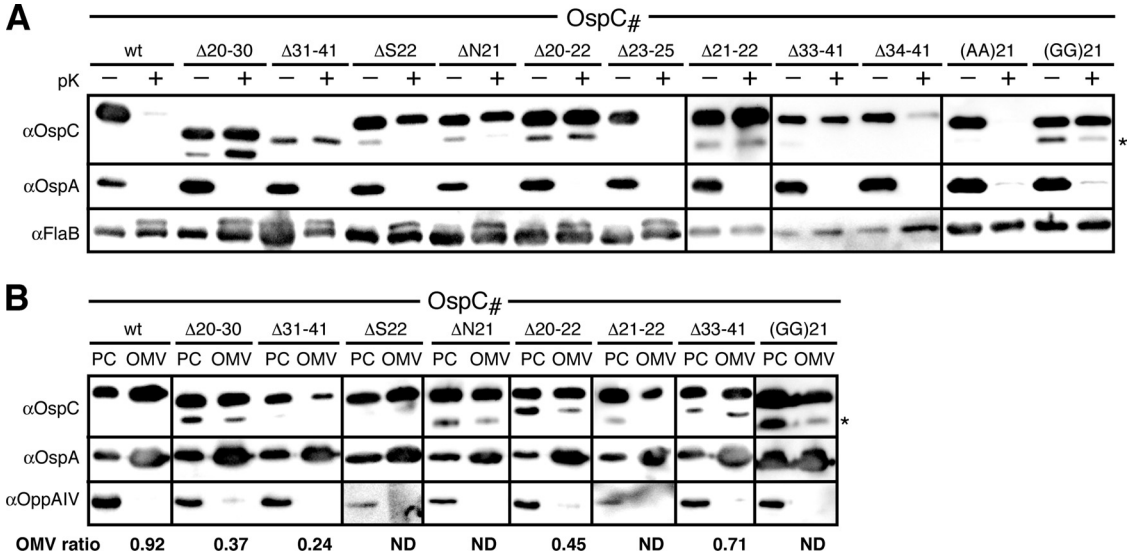

FIG. 3. Localization of OspC mutants. (A) Proteinase K (pK) accessibility immunoblots of OspC tether mutants compared with that of $OspA_{wt}$. FlaB was used as a periplasmic, protease-resistant control. (B) Membrane fractionation immunoblots of proteinase K-resistant, i.e., periplasmic OspC tether mutants compared with that of $OspA_{wt}$. OppAIV served as the IM control. OMV, outer membrane vesicle fraction; PC, protoplasmic cylinder fraction (also containing intact cells) (59, 64). The OMV ratio was calculated from densitometry data that were normalized to both OspA and OppAIV as described previously (31). An asterisk (*) in both panels indicates a CtpA-dependent OspC band (see text) (43) (Kumru et al., submitted).

OspC core protein could therefore serve as a hallmark for a properly folded OspC. To gain access to the periplasmic $OspC_{\Delta 20\text{-}30}$ and $OspC_{\Delta 31\text{-}41}$ proteins, we were required to permeabilize the borrelial envelope with 0.1% SDS (27) prior to trypsin treatment. In the presence of 0.1% SDS, $OspC_{\Delta 20\text{-}30}$ and $OspC_{\Delta 31\text{-}41}$ were terminally cleaved by trypsin-like wild-type OspC ($OspC_{wt}$) (Fig. 6A), resulting in a lower-molecular-weight band. Based on densitometry of Western immunoblot signals, we observed an approximately 2- to 3-fold decrease in $OspC_{\Delta 20\text{-}30}$ and $OspC_{\Delta 31\text{-}41}$ total protein compared to that of $OspC_{wt}$. The trypsin resistance of periplasmic OspC was comparable to that of surface OspA in the presence of detergent and significantly higher than that of periplasmic OM lipoprotein Lp6.6 (Fig. 6A). It is notable that FlaB, under these specific experimental conditions, appears protected from trypsin cleavage; Coomassie staining of SDS-PAGE-fractionated whole-cell protein samples confirmed equal sample loading (not shown). Prior studies indicated that FlaB was susceptible (i) to trypsin after disrupting the cellular architecture by sonication (41) or (ii) to proteinase K after the detergent-based envelope permeabilization protocol described here was used (27). The observed protease resistance of FlaB is therefore likely due to the combination of a gentler envelope disruption procedure with the use of a more specific protease.

In a second experiment, we probed the oligomeric state of periplasmic OspC by formaldehyde cross-linking and *in situ*

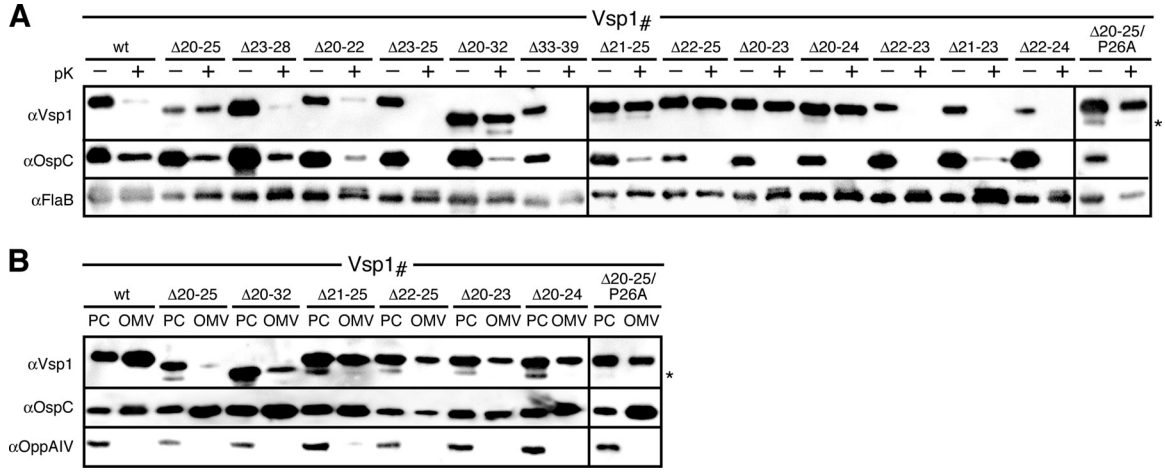

FIG. 4. Localization of Vsp1 mutants. (A) Proteinase K (pK) accessibility immunoblots of Vsp1 tether mutants compared with that of $OspC_{wt}$. FlaB was used as a periplasmic, protease-resistant control. (B) Membrane fractionation immunoblots of proteinase K-resistant, i.e., periplasmic Vsp1 tether mutants compared with that of $OspC_{wt}$. OppAIV served as the IM control. OMV, outer membrane vesicle fraction; PC, protoplasmic cylinder fraction (also containing intact cells) (59, 64). An asterisk (*) in both panels indicates a CtpA-dependent OspC band (see text) (43) (Kumru et al., submitted).

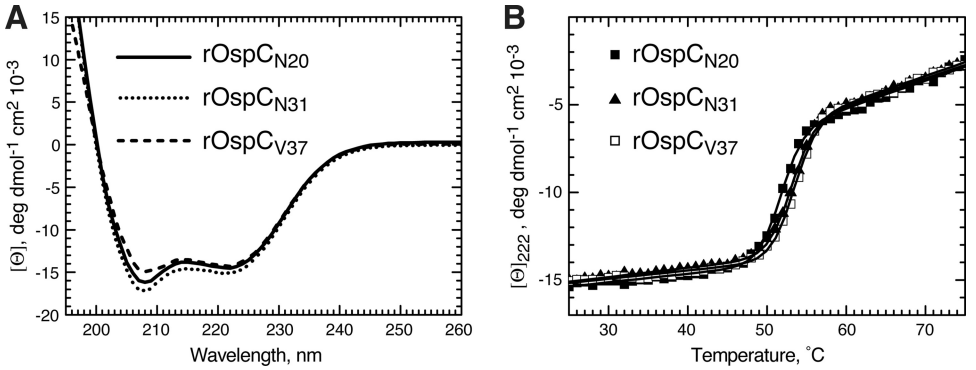

FIG. 5. Circular dichroism and thermal denaturation data for recombinant OspC tether deletion mutants. (A) Circular dichroism spectra of recombinant OspC proteins. Per-residue ellipticity [Θ] plotted as a function of wavelength indicates that all mutants have similar structures dominated by an α-helical conformation. All spectra were obtained at 25°C in 10 mM $NaPO_4$ buffer. (B) Thermal unfolding of rOspC proteins determined as change in ellipticity at 222 nm. Solid lines represent fitting to a two-state transition model. The values for the transition enthalpy (ΔH) and the free energy of the native state (ΔG) (both in kcal/mole), along with the transition temperature (T_m) are shown in Table 3.

surface proteolysis. Upon the addition of formaldehyde, we detected a 46-kDa band corresponding to the OspC dimer (Fig. 6B) (13). The $OspC_{\Delta 20\text{-}30}$ and $OspC_{\Delta 31\text{-}41}$ dimers were protected from proteinase K, indicating their subsurface localization. Based on this evidence, we concluded that mislocalized OspC tether mutants were not blocked from assuming a proper conformation within the periplasm.

Structure destabilization of periplasmic OspC stimulates OM translocation. We previously found that C-terminal epitope tags of the periplasmic $OspA_{\Delta S22}$ mutant were selectively surface exposed (58). To determine if an identically tagged OspC protein would have the same phenotype, we added a C-terminal His tag to $OspC_{\Delta 22}$. To our surprise, not only the C-terminal tag but also the entire $OspC_{\Delta S22}$-His became surface localized (Fig. 7A). Surface proteolysis with trypsin tested for the maintenance of the OspC trypsin-resistant core (19, 30, 75). Cell-associated $OspC_{wt}$, OspC-His, and $OspC_{\Delta S22}$-His proteins showed the expected proteolytic pattern, i.e., a removal of the C terminus (Fig. 7B). The trypsin-resistant core protein released from the cell into the reaction supernatant was clearly detectable for $OspC_{wt}$ but not for the OspC-His and $OspC_{\Delta S22}$-His proteins. This indicated that the addition of a C-terminal epitope tag sufficiently destabilized the OspC structure to stimulate the mutant's release from the periplasm to the spirochetal surface. Together, these experiments further supported our earlier conclusions that trapping of surface lipoproteins within the periplasm is avoided by maintaining unfolded translocation intermediates.

TABLE 3. Biophysical parameters of recombinant OspC tether deletion mutants

Protein	Value (mean ± SD)[a]		
	ΔH	T_m	ΔG
$rOspC_{N20}$	142 ± 8	51.7 ± 0.1	8.8 ± 0.5
$rOspC_{N31}$	146 ± 8	53.3 ± 0.1	9.2 ± 0.4
$rOspC_{V37}$	147 ± 8	53.0 ± 0.1	8.7 ± 0.5

[a] ΔH, transition enthalpy in kcal mole^{-1}; T_m, transition temperature in °C; ΔG, free energy of the native state in kcal mole^{-1}.

OspC and Vsp1 likely traverse the periplasm as monomeric intermediates. If unfolded periplasmic translocation intermediates were universal for surface lipoproteins, oligomerization interfaces of proteins, such as the OspC/Vsp homodimers, would likely be disrupted. Therefore, these proteins would remain monomeric within the periplasm before assuming their final tertiary and quaternary structures on the spirochetal surface. We used two approaches to test this hypothesis. First, we asked whether periplasmic heterodimerization with a wild-type OspC monomer could rescue a mutant subsurface OspC monomer to the bacterial surface. We transformed *B. burgdorferi* strain B313, which endogenously expresses wild-type OspC, with a plasmid that encodes for the periplasmic $OspC_{\Delta 31\text{-}41}$ and $OspC_{\Delta 20\text{-}30}$ mutants, respectively. Based on densitometry of Western blots, there was no shift in the protease accessibility of the mutant OspC proteins in the presence of wild-type OspC and vice versa (Fig. 6C). This indicated that mutant and wild-type OspC proteins failed to interact with each other in the periplasm.

Second, we set out to generate monomeric mutants of OspC and Vsp1 by disrupting intermolecular salt bridges by charge swapping. All OspC mutants either still dimerized or had a null phenotype (Table 4). However, an obtained triple $Vsp1_{D60K/D87K/D150K}$ mutant (Fig. 1B) was instructive. $Vsp1_{D60K/D87K/D150K}$ was likely destabilized, as it was detected at a lower level than $Vsp1_{wt}$. *In situ* formaldehyde cross-linking and protease accessibility experiments showed that $Vsp1_{D60K/D87K/D150K}$ failed to dimerize yet still reached the *B. burgdorferi* surface (Fig. 6D). This showed that dimerization was not required for Vsp1 surface localization. Together, the two experiments provided preliminary evidence for monomeric periplasmic intermediates of oligomeric surface lipoproteins.

DISCUSSION

While major lipoproteins of diderm bacteria generally localize to the periplasmic leaflets of either the IM or OM depending on N-terminal sorting signals recognized by the Lol machinery, the sorting of major lipoproteins in *Borrelia* is

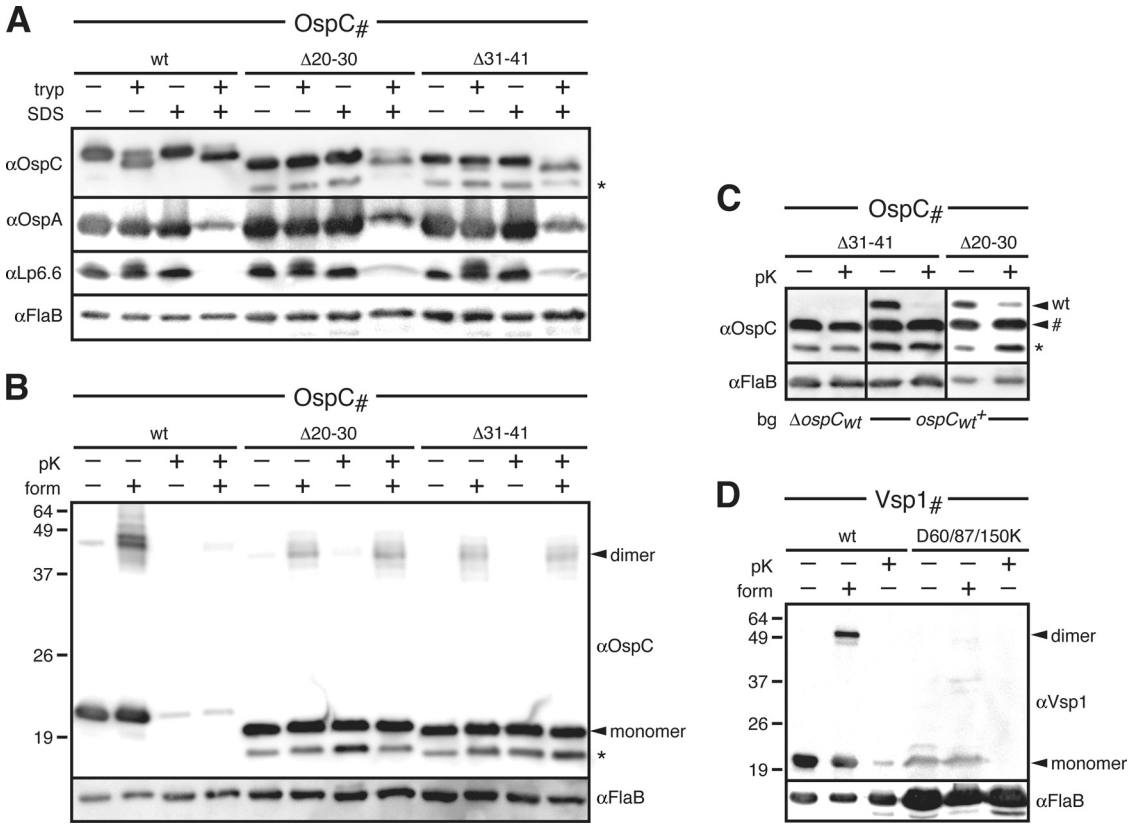

FIG. 6. Structural and functional analysis of select OspC and Vsp1 mutants. (A) Trypsin (tryp) resistance immunoblots of periplasmic OspC tether mutants compared to that of $OspC_{wt}$. Surface $OspA_{wt}$ and periplasmic lipoprotein Lp6.6 were used as OM lipoprotein controls. FlaB was used as a loading control. SDS (0.1%) was used to gain access of trypsin to the periplasm. Note that OspA becomes more susceptible to trypsin in the presence of detergent. (B) Dimerization and proteinase K (pK) accessibility immunoblots of the periplasmic OspC tether mutant compared to that of $OspC_{wt}$. Formaldehyde (form) cross-linking was used to stabilize OspC dimers (13). FlaB was used as both the periplasmic, protease-resistant control and the loading control. (C) Proteinase K (pK) accessibility immunoblots of OspC tether mutants ectopically expressed in an $OspC_{wt}$-deficient (B31-A3 *ospC*::*kan*; Δ*ospC*$_{wt}$) or $OspC_{wt}$-expressing (B313; *ospC*$_{wt}^{+}$) background (bg). Note that there is no reduction in the mutant OspC protein band marked by a pound sign (#) upon protease treatment, independent of the background. FlaB served as a periplasmic, protease-resistant control and a loading control. (D) Dimerization and proteinase K (pK) accessibility immunoblots of the Vsp1 triple salt bridge mutant compared to that of $Vsp1_{wt}$. Formaldehyde (form) cross-linking was used to stabilize any existing Vsp1 dimers (13). FlaB was used as both a periplasmic, protease-resistant control and a loading control. Note that the mutant Vsp1 samples had to be overloaded to sufficiently visualize the Vsp1 monomer. An asterisk (*) in both panels indicates a CtpA-dependent OspC band (see text) (43) (Kumru et al., submitted).

inherently more complex due to the requirement of surface lipoproteins to cross the OM. Our previous studies focused on the secretion requirements of the monomeric surface lipoprotein OspA (58, 59). In the present study, we turned our attention to the *Borrelia* OspC/Vsp lipoproteins, a family of functionally diverse but structurally conserved dimeric surface lipoproteins. This represented an important next step toward our ultimate goal of defining canonical sorting rules for *Borrelia* lipoproteins. It also provided first hints at how *Borrelia* cells cope with an additional layer of complexity during lipoprotein secretion: the oligomerization of dimeric lipoproteins.

Although OspC and Vsp1 share the same protein fold, their overall peptide sequence identity is only about 40% (19, 30, 32, 75). This heterogeneity extends into the membrane-distal tether portions and may explain most of the distinct secretion determinants for the two surface lipoproteins, e.g., the lack of a phenotype for the $Vsp_{\Delta 33\text{-}39}$ mutant. The first five tether residues, however, are conserved between OspC and Vsp1. It is therefore puzzling that the deletion of three residues internal to this pentapeptide yields a subsurface phenotype for $OspC_{\Delta 20\text{-}22}$ but not for $Vsp1_{\Delta 20\text{-}22}$. Deletion of the subsequent tripeptides does not affect surface localization of either $OspC_{\Delta 23\text{-}25}$ or $Vsp1_{\Delta 23\text{-}25}$. This suggests that the Vsp1 Gly^{23}/Thr^{24}/Ser^{25} tripeptide is functionally redundant to Asn^{20}/Asn^{21}/Ser^{22}. However, we cannot exclude that some of the observed variances between OspC and Vsp1 are due to the heterologous expression of Vsp1 in the *B. burgdorferi* surrogate host. While overall lipoprotein sorting mechanisms appear to be conserved within the genus *Borrelia* (76), they might have undergone additional fine-tuning within individual species. Unfortunately, the absence of a genetic system to manipulate *B. turicatae* currently prevents an in-depth experimental exploration of this issue.

Several common attributes are emerging from a comparison of the now known *Borrelia* surface lipoprotein secretion requirements. First, there is the confinement of lipoprotein targeting information to the N-terminal tether peptide. This is not entirely surprising, as the sorting rules previously identified in

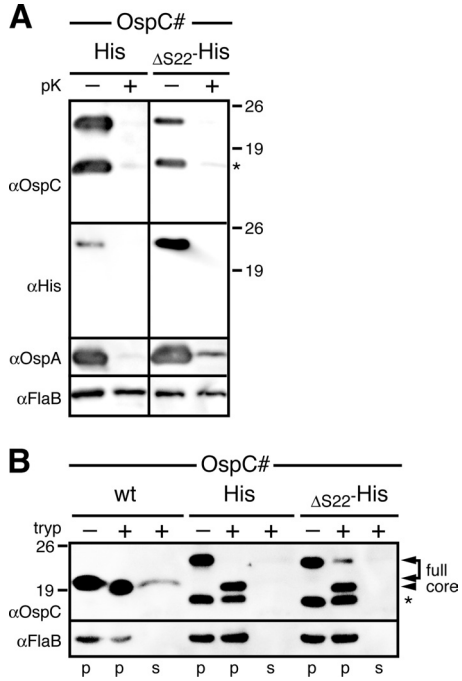

FIG. 7. Structural analysis of epitope-tagged OspC mutants. (A) Proteinase K (pK) accessibility immunoblots of C-terminally histidine-tagged OspC tether mutant $OspC_{\Delta S22}$ compared with that of histidine-tagged $OspC_{wt}$. OspA was used as a surface control, and FlaB was used as a periplasmic, protease-resistant control and a loading control. A HisProbe-HRP (Ni^{2+}-HRP) conjugate was used to confirm the full-length protein band. (B) Trypsin (tryp) resistance immunoblots of C-terminally histidine-tagged OspC tether mutant $OspC_{\Delta S22}$ compared to that of histidine-tagged $OspC_{wt}$ and untagged $OspC_{wt}$. FlaB was used as a loading control. Arrowheads mark the bands corresponding to full-length membrane-associated OspC proteins (full) associating with the cell pellet (p) and trypsin-resistant core proteins (core) released from the cell into the reaction supernatant (s) (75). An asterisk (*) in both panels indicates a CtpA-dependent OspC band (see text) (43) (Kumru et al., submitted).

other diderm bacteria also implicate the N termini of the mature lipoproteins (23, 33, 40, 62, 63, 71). Vsp1/OspC-derived peptides required for the proper secretion of the mRFPΔ4 reporter are at least 3 to 5 residues longer than the OspA minimal tether. This may be a consequence of the above-mentioned optimization of different substrates for a common lipoprotein secretion machinery, and the significance of these length differences may be exaggerated due to the currently limited data set. Second, the essential tether motifs of OspA, OspC, and Vsp1 (shaded in blue in Fig. 1A) commonly contain at least one Ser residue. The significance of this apparent conservation remains to be elucidated. Also conserved is the tolerance for Ala but not Gly substitutions within these motifs of OspA and OspC (Fig. 3) (58). This further supports our earlier conclusions that a defined degree of flexibility within a critical tether segment is required for proper function.

It is worth reiterating that the above-described essential tether motifs are otherwise quite variable in sequence, extent, and spacing relative to the N-terminal acylated cysteine +1 residue. This further bolsters our OspA-based conclusions regarding the absence of a positional +2/+3/+4 rule for *Borrelia* lipoproteins. On first sight, the $Vsp1_{\Delta 20\text{-}25}$ and $Vsp1_{\Delta 20\text{-}25/P26A}$ mutants may provide a counterargument, as they conclusively show that a Pro residue at position +2 specifically leads to lipoprotein mislocalization to the *B. burgdorferi* IM. However, secondary-structure-disrupting prolines are found throughout the tethers of *B. burgdorferi* lipoproteins, except in the +2 position (54, 58). Therefore, a +2 Pro should be considered a nonnative lipoprotein IM retention signal, which interestingly is shared across genus barriers with *E. coli* (62, 68). As such, it might be of questionable biological relevance but may hint at common molecular mechanisms. In the context of our earlier identification of borrelial LolCDE and LolA homologs, as well as basic amino acids serving as borrelial IM retention signals (31, 59, 76), we therefore propose that the lipoprotein sorting mechanisms in the IM of diderm bacteria are conserved on a general level, albeit with variations in the exact nature and placement of the IM retention or Lol avoidance signals.

The current OspC/Vsp1 data also corroborate the previously established OspA-derived requirements for lipoprotein translocation through the OM. First, the ability of a Vsp1 monomer and a structurally destabilized, otherwise periplasmic OspC mutant protein to reach the bacterial surface further supports the requirement of the OM lipoprotein translocation machinery for at least partially unfolded substrates (58). The apparent differences in the phenotypes of C-terminally tagged, otherwise periplasmic OspA and OspC mutants may be explained by the structural differences between the two proteins. In OspA, C-terminal tags are distal from the N-terminal membrane tether and likely will act as separate protein domains. In OspC, however, the proximity of both protein termini may cause the C-terminal tags to sterically interfere with the formation of a tight α-helical bundle. Second, OspC and Vsp1 tether mutants mislocalizing to the periplasm were not prevented from folding and assembling into quaternary structures. However, wild-type OspC molecules failed to rescue mutant mislocalized OspC molecules to the spirochetal surface. This might be due to sequestration of the wild-type protein from its mutant isotype. In light of the other data, however, it is best explained by the failure of wild-type lipoprotein dimer subunits to form proper intermolecular interfaces in the periplasm. Third, the *in vitro* studies of recombinant OspC proteins with various tether deletions demonstrated that the tether peptide did not significantly affect the thermal stability of OspC structure. This suggests that tether peptides of surface lipoproteins, such as OspC, do not possess intrinsic structure-destabilizing proper-

TABLE 4. Phenotypes of OspC/Vsp1 salt bridge charge swap point mutations

Protein	Point mutation(s)	Phenotype
OspC	E61K	Dimer
	E61K/E90K/H93K	Null
	E61K/E90K/H93K/E148K	Null
	E61K/K111A	Dimer
	E61K/E90K/H93K/E148K/K111A	Null
	E90K/H93K/E148K	Dimer
Vsp1	D60K	Dimer
	D60K/D87K	Dimer
	D60K/D87K/D150K	Monomer
	D60K/D87K/D150K/E191K	Null

ties, i.e., they most likely require binding to a "holding" chaperone to prevent premature folding in the periplasm and thereby exclusion from the bacterial surface.

Future studies will continue to define sorting determinants for other mono- and multimeric lipoproteins targeted to different subcellular compartments, test the involvement of the Lol machinery in the secretion of surface lipoproteins, and aim to identify additional lipoprotein secretion pathway components, including the hypothesized OM lipoprotein flippase complex (74). Together, these studies will continually refine our working model of how *B. burgdorferi* targets its most important class of virulence factors to the host-pathogen interface.

ACKNOWLEDGMENTS

This research was supported by NIH grant R01-AI063261 to W.R.Z. and in part by a Graduate Training Program in Multidimensional Vaccinogenesis (NIH T32-AI070089) fellowship to O.S.K. and NIH grant R01-GM069783 to A.S.L.

We thank Catherine Lawson for valuable advice on the structure-based manipulation of OspC and Vsp1, Kit Tilly and Patricia Rosa for the *ospC* knockout strain, and Bob Gilmore for OspC antibodies.

REFERENCES

1. **Akins, D. R., et al.** 1999. Molecular and evolutionary analysis of *Borrelia burgdorferi* 297 circular plasmid-encoded lipoproteins with OspE- and OspF-like leader peptides. Infect. Immun. **67:**1526–1532.
2. **Anguita, J., et al.** 2002. Salp15, an *Ixodes scapularis* salivary protein, inhibits CD4(+) T cell activation. Immunity **16:**849–859.
3. **Babb, K., J. D. McAlister, J. C. Miller, and B. Stevenson.** 2004. Molecular characterization of *Borrelia burgdorferi erp* promoter/operator elements. J. Bacteriol. **186:**2745–2756.
4. **Barbour, A. G.** 1984. Isolation and cultivation of Lyme disease spirochetes. Yale J. Biol. Med. **57:**521–525.
5. **Barbour, A. G., and B. P. Guo.** 2010. Pathogenesis of relapsing fever, p. 333–357. *In* D. S. Samuels and J. D. Radolf (ed.), *Borrelia*: molecular biology, host interaction and pathogenesis. Caister Academic Press, Norwich, United Kingdom.
6. **Barbour, A. G., S. L. Tessier, and W. J. Todd.** 1983. Lyme disease spirochetes and ixodid tick spirochetes share a common surface antigenic determinant defined by a monoclonal antibody. Infect. Immun. **41:**795–804.
7. **Battisti, J. M., et al.** 2008. Outer surface protein A protects Lyme disease spirochetes from acquired host immunity in the tick vector. Infect. Immun. **76:**5228–5237.
8. **Becker, M., et al.** 2005. Structural investigation of *Borrelia burgdorferi* OspB, a bactericidal Fab target. J. Biol. Chem. **280:**17363–17370.
9. **Beena, K., J. B. Udgaonkar, and R. Varadarajan.** 2004. Effect of signal peptide on the stability and folding kinetics of maltose binding protein. Biochemistry **43:**3608–3619.
10. **Bono, J. L., K. Tilly, B. Stevenson, D. Hogan, and P. Rosa.** 1998. Oligopeptide permease in *Borrelia burgdorferi*: putative peptide-binding components encoded by both chromosomal and plasmid loci. Microbiology **144:**1033–1044.
11. **Brandt, M. E., B. S. Riley, J. D. Radolf, and M. V. Norgard.** 1990. Immunogenic integral membrane proteins of *Borrelia burgdorferi* are lipoproteins. Infect. Immun. **58:**983–991.
12. **Braun, V., and K. Rehn.** 1969. Chemical characterization, spatial distribution and function of a lipoprotein (murein-lipoprotein) of the *E. coli* cell wall. The specific effect of trypsin on the membrane structure. Eur. J. Biochem. **10:**426–438.
13. **Bunikis, J., and A. G. Barbour.** 1999. Access of antibody or trypsin to an integral outer membrane protein (P66) of *Borrelia burgdorferi* is hindered by Osp lipoproteins. Infect. Immun. **67:**2874–2883.
14. **Cadavid, D., P. M. Pennington, T. A. Kerentseva, S. Bergström, and A. G. Barbour.** 1997. Immunologic and genetic analyses of VmpA of a neurotropic strain of *Borrelia turicatae*. Infect. Immun. **65:**3352–3360.
15. **Cadavid, D., D. D. Thomas, R. Crawley, and A. G. Barbour.** 1994. Variability of a bacterial surface protein and disease expression in a possible mouse model of systemic Lyme borreliosis. J. Exp. Med. **179:**631–642.
16. **Chen, J. C., P. H. Viollier, and L. Shapiro.** 2005. A membrane metalloprotease participates in the sequential degradation of a *Caulobacter* polarity determinant. Mol. Microbiol. **55:**1085–1103.
17. **Coutte, L., et al.** 2003. Surface anchoring of bacterial subtilisin important for maturation function. Mol. Microbiol. **49:**529–539.
18. **Eftink, M. R., K. J. Helton, A. Beavers, and G. D. Ramsay.** 1994. The unfolding of *trp* aporepressor as a function of pH: evidence for an unfolding intermediate. Biochemistry **33:**10220–10228.
19. **Eicken, C., et al.** 2001. Crystal structure of Lyme disease antigen outer surface protein C from *Borrelia burgdorferi*. J. Biol. Chem. **276:**10010–10015.
20. **Francetic, O., and A. P. Pugsley.** 2005. Towards the identification of type II secretion signals in a nonacylated variant of pullulanase from *Klebsiella oxytoca*. J. Bacteriol. **187:**7045–7055.
21. **Frank, K. L., S. F. Bundle, M. E. Kresge, C. H. Eggers, and D. S. Samuels.** 2003. *aadA* confers streptomycin resistance in *Borrelia burgdorferi*. J. Bacteriol. **185:**6723–6727.
22. **Gandhi, G., et al.** 2010. Interaction of variable bacterial outer membrane lipoproteins with brain endothelium. PLoS One **5:**e13257.
23. **Gennity, J. M., and M. Inouye.** 1991. The protein sequence responsible for lipoprotein membrane localization in *Escherichia coli* exhibits remarkable specificity. J. Biol. Chem. **266:**16458–16464.
24. **Grimm, D., et al.** 2004. Outer-surface protein C of the Lyme disease spirochete: a protein induced in ticks for infection of mammals. Proc. Natl. Acad. Sci. U. S. A. **101:**3142–3147.
25. **Hantke, K., and V. Braun.** 1973. The structure of covalent binding of lipid to protein in the murein-lipoprotein of the outer membrane of *Escherichia coli*. Hoppe-Seylers Z. Physiol. Chem. **354:**813–815.
26. **Ho, S. N., H. D. Hunt, R. M. Horton, J. K. Pullen, and L. R. Pease.** 1989. Site-directed mutagenesis by overlap extension using the polymerase chain reaction. Gene **77:**51–59.
27. **Jewett, M. W., et al.** 2007. Genetic basis for retention of a critical virulence plasmid of *Borrelia burgdorferi*. Mol. Microbiol. **66:**975–990.
28. **Kovacs-Simon, A., R. W. Titball, and S. L. Michell.** 2010. Lipoproteins of bacterial pathogens. Infect. Immun. **79:**548–561.
29. **Kudryashev, M., et al.** 2009. Comparative cryo-electron tomography of pathogenic Lyme disease spirochetes. Mol. Microbiol. **71:**1415–1434.
30. **Kumaran, D., et al.** 2001. Crystal structure of outer surface protein C (OspC) from the Lyme disease spirochete, *Borrelia burgdorferi*. EMBO J. **20:**971–978.
31. **Kumru, O. S., R. J. Schulze, J. G. Slusser, and W. R. Zückert.** 2010. Development and validation of a FACS-based lipoprotein localization screen in the Lyme disease spirochete *Borrelia burgdorferi*. BMC Microbiol. **10:**277.
32. **Lawson, C. L., B. H. Yung, A. G. Barbour, and W. R. Zückert.** 2006. Crystal structure of neurotropism-associated variable surface protein 1 (Vsp1) of *Borrelia turicatae*. J. Bacteriol. **188:**4522–4530.
33. **Lewenza, S., D. Vidal-Ingigliardi, and A. P. Pugsley.** 2006. Direct visualization of red fluorescent lipoproteins indicates conservation of the membrane sorting rules in the family *Enterobacteriaceae*. J. Bacteriol. **188:**3516–3524.
34. **Li, H., J. J. Dunn, B. J. Luft, and C. L. Lawson.** 1997. Crystal structure of Lyme disease antigen outer surface protein A complexed with an Fab. Proc. Natl. Acad. Sci. U. S. A. **94:**3584–3589.
35. **Liu, G., T. B. Topping, and L. L. Randall.** 1989. Physiological role during export for the retardation of folding by the leader peptide of maltose-binding protein. Proc. Natl. Acad. Sci. U. S. A. **86:**9213–9217.
36. **Magoun, L., et al.** 2000. Variable small protein (Vsp)-dependent and Vsp-independent pathways for glycosaminoglycan recognition by relapsing fever spirochaetes. Mol. Microbiol. **36:**886–897.
37. **Matsuyama, S., T. Tajima, and H. Tokuda.** 1995. A novel periplasmic carrier protein involved in the sorting and transport of *Escherichia coli* lipoproteins destined for the outer membrane. EMBO J. **14:**3365–3372.
38. **Matsuyama, S., N. Yokota, and H. Tokuda.** 1997. A novel outer membrane lipoprotein, LolB (HemM), involved in the LolA (p20)-dependent localization of lipoproteins to the outer membrane of *Escherichia coli*. EMBO J. **16:**6947–6955.
39. **Mbow, M. L., R. D. J. Gilmore, and R. G. Titus.** 1999. An OspC-specific monoclonal antibody passively protects mice from tick-transmitted infection by *Borrelia burgdorferi* B31. Infect. Immun. **67:**5470–5472.
40. **Narita, S., and H. Tokuda.** 2007. Amino acids at positions 3 and 4 determine the membrane specificity of *Pseudomonas aeruginosa* lipoproteins. J. Biol. Chem. **282:**13372–13378.
41. **Noppa, L., Y. Östberg, M. Lavrinovicha, and S. Bergström.** 2001. P13, an integral membrane protein of *Borrelia burgdorferi*, is C-terminally processed and contains surface-exposed domains. Infect. Immun. **69:**3323–3334.
42. **Norris, S. J., J. Coburn, J. M. Leong, L. T. Hu, and M. Höök.** 2010. Pathobiology of Lyme disease *Borrelia*, p. 299–332. *In* D. S. Samuels and J. D. Radolf (ed.), *Borrelia*: molecular biology, host interaction and pathogenesis. Caister Academic Press, Norwich, United Kingdom.
43. **Östberg, Y., et al.** 2004. Pleiotropic effects of inactivating a carboxyl-terminal protease, CtpA, in *Borrelia burgdorferi*. J. Bacteriol. **186:**2074–2084.
44. **Pal, U., et al.** 2000. Attachment of *Borrelia burgdorferi* within *Ixodes scapularis* mediated by outer surface protein A. J. Clin. Invest. **106:**561–569.
45. **Pal, U., et al.** 2004. TROSPA, an *Ixodes scapularis* receptor for *Borrelia burgdorferi*. Cell **119:**457–468.
46. **Pal, U., et al.** 2001. Inhibition of *Borrelia burgdorferi*-tick interactions *in vivo* by outer surface protein A antibody. J. Immunol. **166:**7398–7403.
47. **Park, S., G. Liu, T. B. Topping, W. H. Cover, and L. L. Randall.** 1988. Modulation of folding pathways of exported proteins by the leader sequence. Science **239:**1033–1035.
48. **Pennington, P. M., C. D. Allred, C. S. West, R. Alvarez, and A. G. Barbour.**

1997. Arthritis severity and spirochete burden are determined by serotype in the *Borrelia turicatae*-mouse model of Lyme disease. Infect. Immun. **65:**285–292.
49. **Pennington, P. M., D. Cadavid, and A. G. Barbour.** 1999. Characterization of VspB of *Borrelia turicatae*, a major outer membrane protein expressed in blood and tissues of mice. Infect. Immun. **67:**4637–4645.
50. **Potterton, E., S. McNicholas, E. Krissinel, K. Cowtan, and M. Noble.** 2002. The CCP4 molecular-graphics project. Acta Crystallogr. D Biol. Crystallogr. **58:**1955–1957.
51. **Pugsley, A. P.** 1993. The complete general secretory pathway in Gram-negative bacteria. Microbiol. Rev. **57:**50–108.
52. **Pugsley, A. P., M. G. Kornacker, and A. Ryter.** 1990. Analysis of the subcellular location of pullulanase produced by *Escherichia coli* carrying the *pulA* gene from *Klebsiella pneumoniae* strain UNF5023. Mol. Microbiol. **4:**59–72.
53. **Ramamoorthi, N., et al.** 2005. The Lyme disease agent exploits a tick protein to infect the mammalian host. Nature **436:**573–577.
54. **Robertson, A. D., and K. P. Murphy.** 1997. Protein structure and the energetics of protein stability. Chem. Rev. **97:**1251–1268.
55. **Sadziene, A., D. D. Thomas, and A. G. Barbour.** 1995. *Borrelia burgdorferi* mutant lacking Osp: biological and immunological characterization. Infect. Immun. **63:**1573–1580.
56. **Sadziene, A., B. Wilske, M. S. Ferdows, and A. G. Barbour.** 1993. The cryptic *ospC* gene of *Borrelia burgdorferi* B31 is located on a circular plasmid. Infect. Immun. **61:**2192–2195.
57. **Sauvonnet, N., and A. P. Pugsley.** 1996. Identification of two regions of *Klebsiella oxytoca* pullulanase that together are capable of promoting beta-lactamase secretion by the general secretory pathway. Mol. Microbiol. **22:** 1–7.
58. **Schulze, R. J., S. Chen, O. S. Kumru, and W. R. Zückert.** 2010. Translocation of *Borrelia burgdorferi* surface lipoprotein OspA through the outer membrane requires an unfolded conformation and can initiate at the C terminus. Mol. Microbiol. **76:**1266–1278.
59. **Schulze, R. J., and W. R. Zückert.** 2006. *Borrelia burgdorferi* lipoproteins are secreted to the outer surface by default. Mol. Microbiol. **59:**1473–1484.
60. **Schwan, T. G., and J. Piesman.** 2000. Temporal changes in outer surface proteins A and C of the Lyme disease-associated spirochete, *Borrelia burgdorferi*, during the chain of infection in ticks and mice. J. Clin. Microbiol. **38:**382–388.
61. **Schwan, T. G., J. Piesman, W. T. Golde, M. C. Dolan, and P. A. Rosa.** 1995. Induction of an outer surface protein on *Borrelia burgdorferi* during tick feeding. Proc. Natl. Acad. Sci. U. S. A. **92:**2909–2913.
62. **Seydel, A., P. Gounon, and A. P. Pugsley.** 1999. Testing the '+2 rule' for lipoprotein sorting in the *Escherichia coli* cell envelope with a new genetic selection. Mol. Microbiol. **34:**810–821.
63. **Silva-Herzog, E., F. Ferracci, M. W. Jackson, S. S. Joseph, and G. V. Plano.** 2008. Membrane localization and topology of the *Yersinia pestis* YscJ lipoprotein. Microbiology **154:**593–607.
64. **Skare, J. T., et al.** 1995. Virulent strain associated outer membrane proteins of *Borrelia burgdorferi.* J. Clin. Invest. **96:**2380–2392.
65. **Srivastava, S. Y., and A. M. de Silva.** 2008. Reciprocal expression of *ospA* and *ospC* in single cells of *Borrelia burgdorferi*. J. Bacteriol. **190:**3429–3433.
66. **Stevenson, B., T. G. Schwan, and P. A. Rosa.** 1995. Temperature-related differential expression of antigens in the Lyme disease spirochete, *Borrelia burgdorferi*. Infect. Immun. **63:**4535–4539.
67. **Stewart, P. E., R. Thalken, J. L. Bono, and P. Rosa.** 2001. Isolation of a circular plasmid region sufficient for autonomous replication and transformation of infectious *Borrelia burgdorferi*. Mol. Microbiol. **39:**714–721.
68. **Tokuda, H., S. Matsuyama, and K. Tanaka-Masuda.** 2007. Structure, function, and transport of lipoproteins in *Escherichia coli*, p. 67–79. *In* M. Ehrmann (ed.), The periplasm. ASM Press, Washington, DC.
69. **van Ulsen, P., et al.** 2003. A neisserial autotransporter NalP modulating the processing of other autotransporters. Mol. Microbiol. **50:**1017–1030.
70. **Yakushi, T., K. Masuda, S. Narita, S. Matsuyama, and H. Tokuda.** 2000. A new ABC transporter mediating the detachment of lipid-modified proteins from membranes. Nat. Cell Biol. **2:**212–218.
71. **Yamaguchi, K., F. Yu, and M. Inouye.** 1988. A single amino acid determinant of the membrane localization of lipoproteins in *E. coli*. Cell **53:**423–432.
72. **Yokota, N., T. Kuroda, S. Matsuyama, and H. Tokuda.** 1999. Characterization of the LolA-LolB system as the general lipoprotein localization mechanism of *Escherichia coli*. J. Biol. Chem. **274:**30995–30999.
73. **Zückert, W. R.** 2007. Laboratory maintenance of *Borrelia burgdorferi*. Curr. Protoc. Microbiol. **12:**12C.1.
74. **Zückert, W. R., and S. Bergström.** 2010. Structure, function and biogenesis of the *Borrelia* cell envelope, p. 139–166. *In* D. S. Samuels and J. D. Radolf (ed.), *Borrelia*: molecular biology, host interaction and pathogenesis. Caister Academic Press, Norwich, United Kingdom.
75. **Zückert, W. R., T. A. Kerentseva, C. L. Lawson, and A. G. Barbour.** 2001. Structural conservation of neurotropism-associated VspA within the variable *Borrelia* Vsp-OspC lipoprotein family. J. Biol. Chem. **276:**457–463.
76. **Zückert, W. R., J. E. Lloyd, P. E. Stewart, P. A. Rosa, and A. G. Barbour.** 2004. Cross-species surface display of functional spirochetal lipoproteins by recombinant *Borrelia burgdorferi*. Infect. Immun. **72:**1463–1469.
77. **Zückert, W. R., J. Meyer, and A. G. Barbour.** 1999. Comparative analysis and immunological characterization of the *Borrelia* Bdr protein family. Infect. Immun. **67:**3257–3266.